SAND2019-6964C

Geographic Assessment of Photovoltaic Module Environmental Degradation Stressors

C. Birk Jones *, Todd Karin †, Anubhav Jain †,William B. Hobbs ‡, and Cara Libby §

*Sandia National Laboratories, Albuquerque, NM, U.S.A
†Lawrence Berkeley National Laboratory, Berkeley, CA, U.S.A
‡Southern Company, Birmingham, AL, U.S.A
§Electric Power Research Institute, Palo Alto, CA, U.S.A

***Abstract*—This work identifies and plots the environmental stressors that are known to degrade photovoltiac (PV) modules. The literature search identifies models that estimate the damage caused by a PV modules exposure to various weather, including temperature, radiation, and humidity. The weather related variables are identified and plotted using contour plots to highlight the geographic distribution across the U.S. In this case, we used the Global Land Data Assimilation System (GLDAS) to plot ambient temperature, irradiance, and specific humidity. The analysis also calculated the degradation model stressors using the GLDAS data set (i.e. module temperature, plane of array irradiance, and relative humidity) and compared these values with the standard variables to identify correlations and required translation to represent the stressor accurately. The results show that global horizontal (GHI) irradiance provides a sufficient representation, module temperature at GHI needs to be calculated, and specific humidity is significantly different from relative humidity.**

***Index Terms*—photovoltaic, accelerated aging, series resistance**

I. Introduction

The potential exposure of photovoltaic (PV) modules to environmental stressors in different geographic regions is assessed using the Global Land Data Assimilation System (GLDAS) data set [1]. Exposure to extreme temperatures [2], humidity [3], thermal cycling [4], ultraviolet (UV) radiation, and others can stress and damage the bonds, packaging, electrical components, and the solar cells of photovoltaic (PV) modules. The GLDAS data set's weather variables (e.g. ambient temperature, radiation, etc.) provides a qualitative review of the spatial distribution for environmental stressors in the U.S. Findings from this work can define regional differences, which will lead to PV specific climate zone designations.

The PV industry lacks a well defined climate assessment criteria, whereas other industries use climate maps to define design criteria. For example, the structural engineering field uses geographic climate information to define specific regional wind and snow load parameters. Or, the road pavement industry's temperature zone map helps designers specify layer sizes and mixes for particular regions [5]. It is unclear to what extent the PV industry considers climate when designing modules.

PV researchers and practitioners often cite the Köppen Geiger climate zone map [6]. However, the Köppen Geiger system, developed by Wladimir Köppen in the early 1900s, is based on precipitation and temperature patterns only [7]. The approach created categories for different varieties of vegetation and not for understanding potential long-term impacts on PV module performance. This paper attempts to identify and map environmental stressors that are known to degrade PV modules and inform future development of a climate zone mapping system.

This research paper identifies known stressor variables, calculates and compares them with variables in the GLDAS data set, and evaluates the spatial distribution of each stressor variable. The literature search (Section II) provides a review of degradation models when subjected to accelerated-aging test chamber experiments and outdoor environments. The stressor variables are assessed using the GLDAS data by caclulating, comparing, and maping solar radiation, temperature, and humidity (Section III).

II. Background - Photovoltaic Module Stressors

Abiotic factors, such as temperature, changes in temperature, moisture, module deformation caused by wind, and solar radiation, impact long-term PV performance. Each region in the U.S. experiences these factors at different levels. Past literature considered the exposure to various factors and created formulas to model the impacts. The overview paper [8] documents many of the methods.

A. Solar Radiation

A direct estimate of UV exposure is difficult to measure in the field. However, according to [9], short wave solar irradiance can provide a basic estimate based on Equation 1:

$$D_{uv}(t) = \int_a^b E(u)(0.05)\,\mathrm{d}u. \tag{1}$$

where D_{uv} was the UV dose and E was the total light spectrum solar radiation. In this case, the stressor variable is E.

B. Temperature

Exposure to high module temperature can causes the PV module to degrade the encapsulant, which results in a reduction in electrical current output. Equation 2 provides an estimate of the damage caused by module temperature exposure:

$$D = \mathrm{T}_m \exp\left(\frac{-Q_a}{k_b \mathrm{T}_m}\right) \tag{2}$$

Sandia National Laboratories is a multimission laboratory managed and operated by National Technology & Engineering Solutions of Sandia, LLC, a wholly owned subsidiary of Honeywell International Inc., for the U.S. Department of Energy's National Nuclear Security Administration under contract DE-NA0003525.

where T_m is the maximum temperature, t is the time step, the activation energy Q_a is set to 0.622, and k_b is the Boltzmann constant [10]. Another method, documented in past work, equates the variable module temperature data to a single value that represents the potential exposure if the module had been subjected to a constant temperature over the same time period [11]. This equivalent temperature is calculated using Equation 3:

$$\exp\left(\frac{-Q_a}{k_b T_{eq}}\right) = \frac{1}{t_1 - t_2}\int \exp\left(\frac{-Q_a}{k_b T(t)}\right) dt. \quad (3)$$

where t is the time, and T_{eq} is the equivalent temperature. Each of these equations use module temperature as the stressor variable.

C. Thermal Cycling

Research focused on thermal cycling evaluates the potential damage to the solder bond interconnections. For example, Vasudevan and Fan implements an acceleration factor formula that compares the field and test samples as shown in Equation 4:

$$AF = \left(\frac{f_{field}}{f_{test}}\right)^{-m}\left(\frac{\Delta T_{field}}{\Delta T_{test}}\right)^{-n} \exp\left(\frac{Q_a}{k}\left(\frac{1}{T_{\text{field}}} - \frac{1}{T_{\text{test}}}\right)\right) \quad (4)$$

where f is the thermal cycling frequency, ΔT is the change in temperature, T is the maximum temperature, and "field" and "test" stand for the in-field and indoor test chamber environments [12]. In other work, Bosco et *al.* uses Equation 4 to derive an equation that estimates material damage [13]. In this work, the stress imposed on the solder bond is estimated on Equation 5:

$$D = C(\Delta T)^n (r(T))^m \exp\left[\frac{-Q}{k_B T_{max}}\right] \quad (5)$$

where C is a scaling constant, T_{max} is the average maximum module temperature, ΔT is the mean daily maximum temperature change, and r(T) is the number of times the temperature crossed a threshold. The two thermal cycling damage estimates consider the module temperature as the stressor variable.

D. Humidity

Past literature uses relative humidity (RH) to estimate the degradation caused by moisture. The approach implments a formula known as the Peck equation described in Equation 6:

$$R_{D,Peck} = A\ \exp\left(\frac{-Q_a}{k_b Tm_{max}}\right) RH^n \quad (6)$$

where RH is the relative humidity, Q_a is the activation energy set to 0.49, k_b is Boltzmann's constant, Tm_{max} is the maximum module temperature, and the constants A and n were set to 0.0037 and 3.82 respectively [14]. A similar formula, known as the Eyring model uses the RH variable as well to estimate the module's degradation [14]:

$$R_{D,Eyring} = A\ \exp\left(\frac{-Q_a}{k_b Tm_{max}} - \frac{b}{RH}\right) RH^n \quad (7)$$

III. Methodology

This experiment evaluates the degradation stressors spatial distribution in the U.S. using the GLDAS data set. The evaluation begins with a comparison of the GLDAS variables with the features in the degradation model equations; indirect matches requires the implementation of a translation that calculates the degradation stressor from the GLDAS variables (i.e. ambient temperature to module temperature). Then, the original GLDAS variables are compared with the translations using the contour maps to identify correlations. This evaluation defines which translations are necessary for creating climate zone classification schemes.

A. Data

The GLDAS is an environmental data set for land masses throughout the world. The data set uses land surface models and actual data to generate accurate weather states. For this work, the 0.25-degree resolution maps provides an assessment of the U.S. climate for 2015 and 2016 calendar years. The comparison calculations, such as the plane of array (POA) irradiance, did not include the high resolution data and instead reduced the data set to decrease computational time. The POA estimate is computationally cumbersome because of the angle of incidence (AOI) calculation.

B. Environmental Variables

The environmental variables present in the degradation model equations, described in Section II, do not correspond directly with the GLDAS data set. Therefore, the stressor variables require a translation to convert global horizontal (E_{POA}) irradiance to plane of array irradiance (E_{POA}), and ambient temperature (T_a) to module temperature (T_m). Also, the GLDAS data set does not include RH, and instead provides specific humidity (SH). Therefore, the experiment calculates the RH based on SH, pressure, and T_a. These variables and a general overview of their associated functions are summarized in Table I:

TABLE I
DEGRADATION & GLDAS VARIABLES

No.	Degradation Variable	GLDAS Translation
1	Global Horizontal Irrad.	$E_{POA} = f$(sun & PV angles, E_{GHI})
2	Module Temperature	$T_m = f$(E, Wind, T_a)
3	Relative Humidity	RH = f(T_a,Specific Hum., Pressure)

C. Stressor Contour Maps

The geographic assessment of PV degradation stressors includes the creation and evaluation of contour maps. The maps compare the spatial diversity across the U.S for environmental variables available in the GLDAS data set (i.e. global horizontal irradiance, ambient temperature, and specific humidity) with the PV degradation variables as defined by past research (i.e. solar radiation, module temperature, and relative humidity). The solar radiation maps consider both the GLDAS Global Horizontal (GHI) data and the calculated POA.

1) Solar Radiation: The GLDAS solar radiation variable is described as short wave radiation on a horizontal surface. This equates to the E_{GHI} shown in Figure 1. However, the E_{POA} provides a more accurate representation of the amount of exposure to solar radiation. Therefore, the present work calculates the E_{POA} based on Equation 8:

$$E_{POA} = (E_{DNI})(\cos(AOI)) \tag{8}$$

where E_{DNI} is the direct normal irradiance, and AOI is the angle of incidence. The AOI calculation used the Python PVLIB function that considered the solar azimuth and zenith angles associated with the sun and the array's angles [15], [16]. The E_{DNI} component estimate used Equation 9:

$$E_{DNI} = (E_{GHI} - E_{DHI})/(\cos(Z)) \tag{9}$$

where E_{DHI} is the modeled diffuse horizontal irradiance, and Z is the solar zenith angle. The E_{DHI} estimate is based on the multiplication of the diffuse fraction [17] times the E_{GHI}. The experiment assumed that the modules faced due south and had a tilt angle that was equal to its latitude.

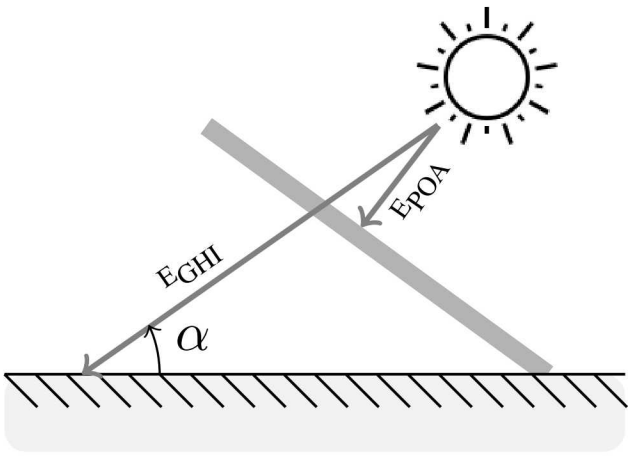

Fig. 1. The GLDAS data set provides the global horizontal irradiance (E_{GHI}). The estimate of the plane of array irradiance (E_{POA}), which is the radiation perpendicular to the solar modules, required the E_{GHI}, as well as the sun and PV module angles.

2) Temperature: The degradation of PV modules depends on the internal temperature and the changes in temperature. However, the module temperature values are not provided by standard data sets and estimates required the implementation of Equation 10 [18]:

$$T_m = E[\exp(a + bW)] + T_a \tag{10}$$

where E is the irradiance, W is the wind, and T_a is the ambient temperature. The constants a and b, which are empirical determined for different module types and mounting configurations, were set to be -3.47 and -0.0594 for an open rack glass on glass module type [18]. The wind and ambient temperatures come from the GLDAS data set. In this work, the E_{POA} and E_{GHI} are used to estimate the respective module temperatures, which are refered to as $T_{m_{POA}}$ and $T_{m_{GHI}}$.

3) Humidity: The evaluation of humidity compares the SH with the estimated RH. SH is the mass of water vapor in a unit of moist air. The RH defines the amount of water vapor that is present in air depending on the temperature. RH is be expressed as the ratio that compares the specific mass of water vapor with the specific mass of dry air:

$$RH = \frac{m_v}{m_d} \approx 0.622\frac{e_s}{p} \tag{11}$$

where m_v is the specific mass of water vapor, m_d is the specific mass of dry air, e_s is the saturation vapor pressure, and p is the atmospheric pressure. The saturation vapor pressure can be estimated using Equation 12:

$$e_s \approx 611 \cdot \exp\left(\frac{17.67(T - T_o)}{T - 29.65}\right) \tag{12}$$

where T is the ambient temperature in kelvin and T_o is the reference temperature that was set to be 273.15 K. The saturation vapor pressure equation (Equation 12) was plugged into Equation 11 and the resulting function to calculate RH is shown in Equation 13:

$$RH = 0.26(P)(SH)\left[\exp\left(\frac{17.67(T - T_o)}{T - 29.65}\right)\right]^{-1} \tag{13}$$

where P is the atmospheric pressure, and SH is the specific humidity.

The experiment compares the specific humidity with relative humidity to identify key differences that could impact the review of the degradation stressor across the U.S. Since the two metrics use different units, each are converted to a normalized value between 0 and 1 as described by Equation 14:

$$n_x = \frac{x - \max(x)}{\max(x) - \min(x)} \tag{14}$$

where x is the humidity variable, and n_x is the normalized variable.

IV. Results

The results section describes the geographic climate trends for solar radiation (Section IV-A), temperature (Section IV-B), and humidity (Section IV-C).

A. Solar Radiation

The average E_{GHI} is plotted in Figure 2. The highest amount of radiation is in the southwest and decreases to the north, northeast, and east. The radiation is also high in the southwestern part of Florida. The comparison between the GLDAS provided E_{GHI} and the calculated E_{POA} identifies differences that are different across the U.S.

The difference between the E_{GHI} and E_{POA} ranged between -2 to 80 W/m^2 (-6% and 30%) across the U.S. The contour plot in Figure 3 indicates that the largest difference occurres in the south and decreases to the north. Areas in the south part of the country has differences of about 16-32W/m^2 and reaches as high as 80W/m^2 in Mexico. The middle latitudes had smaller differences that ranged between 5 and 16W/m^2. The north has a calculated E_{POA} greater than

the E_{GHI}, and thus the difference drops slightly below zero. The relatively low differences imply that the E_{GHI} represents the spatial distribution for irradiance well.

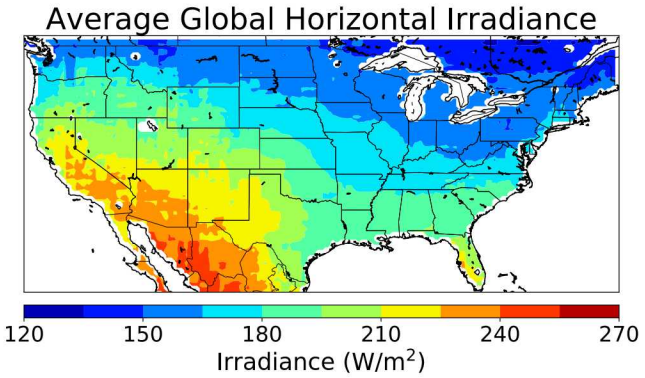

Fig. 2. Average annual global horizontal irradiance shows high values in the southwest that decreases to the north, east, and northeast.

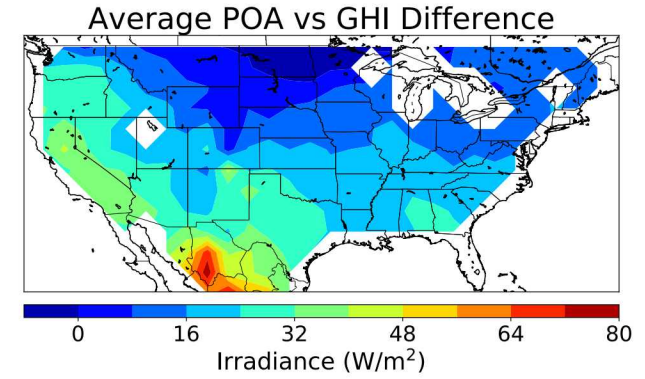

Fig. 3. The difference in plane of array and global horizontal irradiance varied across the U.S. The southern part of the country has larger differences, while the north had smaller values that are near zero and negative in the far north.

B. Temperature

The average T_a varies across the U.S. as shown in Figure 4. The hottest locations tend to be in the south along the Gulf of Mexico and in the west near the boarder of Arizona and California. As expected, the Rocky Mountains and the far northeast states had the coldest average temperatures. However, T_a is not a variable in the temperature and thermal cycling degradation models. Therefore, Section IV-B1 and IV-B2 compare T_a with $T_{m_{POA}}$, and identify the resemblances between $T_{m_{GHI}}$ and $T_{m_{POA}}$ respectively.

1) POA Module vs Ambient Temperature: The difference between T_a and $T_{m_{POA}}$ ranges between -6°C and -3°C as shown in Figure 5. The largest differences occur in the southwest and decrease to the northeast. The southwest experiences a larger discrepancy between the $T_{m_{POA}}$ and T_a because of the high solar radiation present in that region. Furthermore, the overall bias is linked to the impact of irradiance on the module temperature that does not effect T_a as much. The general bias, and range of differences suggest that T_a does not correlate well with the $T_{m_{POA}}$. The next section compares the module temperature calculated using GHI and POA irradiance.

2) POA vs GHI Module Temperature: The difference in module temperature based on E_{GHI} and E_{POA} inputs, shown in Figure 6, ranged from -0.3 to 2.4°C. This contour plot resembles the map that compares POA and GHI irradiance (Figure 3). Both contour maps have differences that are low and below zero in the north, and shift to be larger and

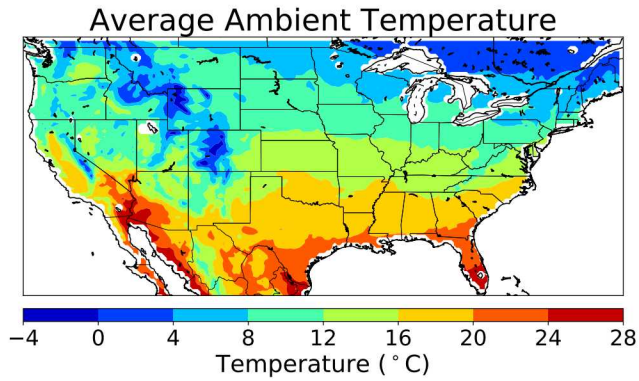

Fig. 4. Average annual ambient temperature across the U.S.

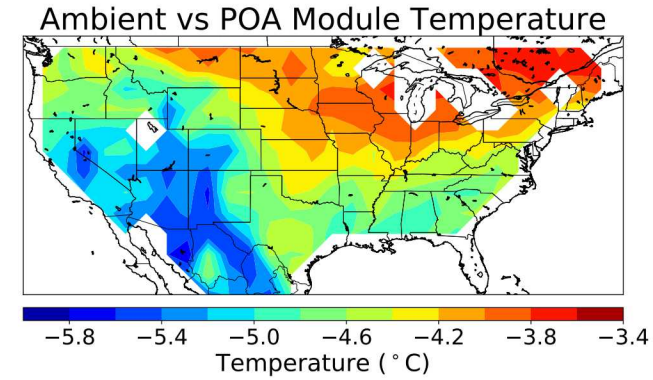

Fig. 5. The difference in module temperature (at POA) and ambient temperature was larger in the southwest and smaller in the northeast.

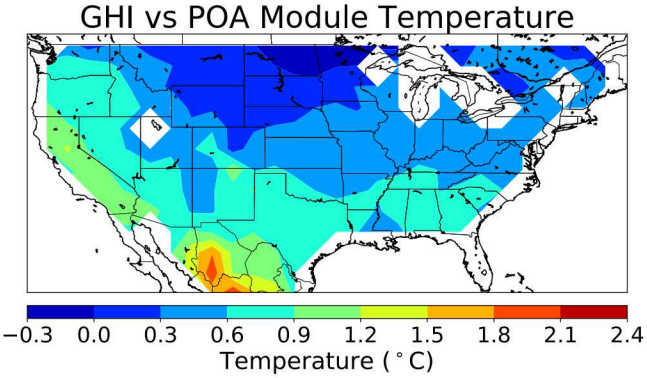

Fig. 6. The difference in module temperature based on GHI and POA irradiance varied across the U.S. In the north, the difference was small and slightly below zero. In the south the difference ranged between 0.3 to 1.2°C.

above zero in the southern part of the country. The small differences suggest that $T_{m_{GHI}}$ provides a reasonable estimate of a modules temperature throughout the U.S.

C. Humidity

The humidity analysis identifies spatial differences between SH and RH. The contour plots for each humidity metric are plotted in Figures 7 and 8. The SH map, in Figure 7, indicates that there are significant amounts of moisture along the Gulf Coast that decreases steadily to the north, northwest, and west. Similarly, the RH has the highest values in the southeast region as shown in Figure 8. In contrast, the west part of the country experiences relatively low, and constant SH; the RH is more spatially diverse in this same area.

The similarities and differences between the specific and relative humidity are evident in Figure 9. The comparison showed that the southern part of the country has similar SH and RH. However, the SH and RH diverges in the northeastern region of the country because SH is spatially diverse while the RH is relativley constant in this area. Similarly, in the northwest, the SH is very low and tends to remain the same throughout the region, whereas the RH varies. Lastly, the contour map identifies that the most significant differences

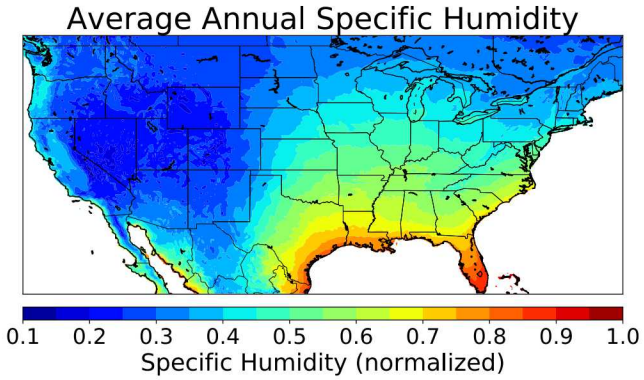

Fig. 7. Normalized specific humidity contour map shows that the southeast has high humidity, while most of the west experiences very low humidity.

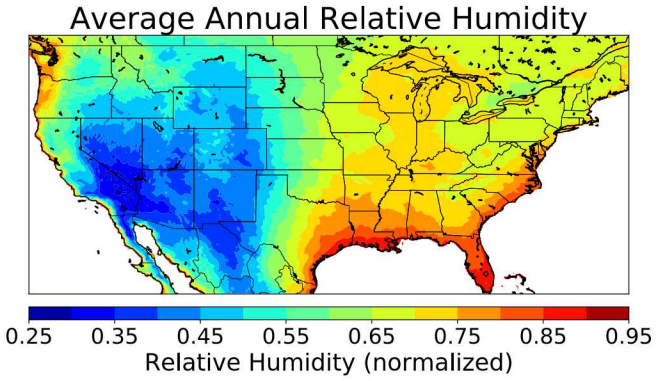

Fig. 8. The normalized relative humidity contour map indicates that the southeast has high humidity and the west is lower but spatial diverse compared to the specific humidity.

are in the high altitudes of the Rocky Mountains and Sierra Nevadas. As a result, the SH does not correlate well with RH. However, it is unclear why RH is used instead of SH since SH provides a better metric for understanding the amount of water present in the air.

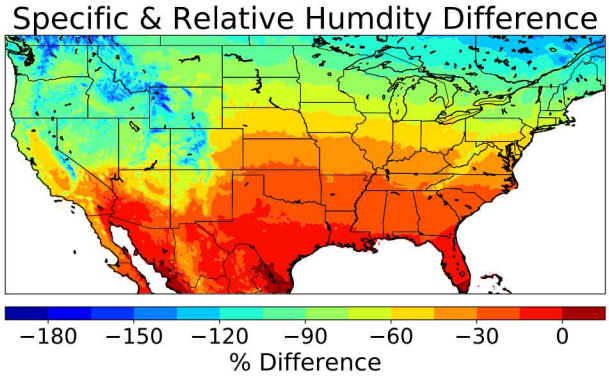

Fig. 9. Normalized difference in average annual specific and relative humidity showed that the southern part of the country had similar results and diverged significantly in the north.

V. Conclusion

This paper evaluates the spacial distribution of environmental stressors in the U.S. The GLDAS data set, which provides ambient temperature, irradiance, and specific humidity to estimate the stressor variables used in past literature to estimate degradation damage. Contour maps provided a review of the spacial distribution of the environmental stressors (module temperature, irradiance, and humidity). The maps showed the differences between the GLDAS data and the computed stressor variables.

The analysis showed that the GLDA data set alone works for certain stressors but not all. The POA irradaince, used in the estimate of UV degradation, can be represented using GHI. However, the ambient temperature, provided by GLDAS, does not correlate well with the module temperature and therefore the calculation of module temperature is required. The past work used relative humidity to estimate the impact of moisture on module degradation. Relative humidity, however, does not match well with the GLDAS provided specific humidity.

The results from this work can provides a basic review of stressors used to model PV degradation and identifies the available data that can represent the stressors geographically. Other work can use the available data to develop climate zone classifications that are specific to PV degradation.

Acknowledgment

This material is based upon work supported by the U.S. Department of Energy's Office of Energy Efficiency and Renewable Energy (EERE) under Solar Energy Technologies Office (SETO) Agreement Number DE-EE0007137.

This paper describes objective technical results and analysis. Any subjective views or opinions that might be expressed in

the paper do not necessarily represent the views of the U.S. Department of Energy or the United States Government.

Sandia National Laboratories is a multi-mission laboratory managed and operated by National Technology and Engineering Solutions of Sandia, LLC., a wholly owned subsidiary of Honeywell International, Inc., for the U.S. Department of Energy's National Nuclear Security Administration under contract DE-NA0003525.

REFERENCES

[1] M. Rodell, P. R. Houser, U. Jambor, J. Gottschalck, K. Mitchell, C.-J. Meng, K. Arsenault, B. Cosgrove, J. Radakovich, M. Bosilovich, J. K. Entin, J. P. Walker, D. Lohmann, and D. Toll, "The Global Land Data Assimilation System," *Bulletin of the American Meteorological Society*, vol. 85, no. 3, pp. 381–394, Mar. 2004. [Online]. Available: https://journals.ametsoc.org/doi/abs/10.1175/BAMS-85-3-381

[2] F. Kersten, P. Engelhart, H.-C. Ploigt, A. Stekolnikov, T. Lindner, F. Stenzel, M. Bartzsch, A. Szpeth, K. Petter, J. Heitmann, and J. W. Mller, "Degradation of multicrystalline silicon solar cells and modules after illumination at elevated temperature," *Solar Energy Materials and Solar Cells*, vol. 142, pp. 83–86, Nov. 2015. [Online]. Available: http://www.sciencedirect.com/science/article/pii/S0927024815002846

[3] M. D. Kempe and J. H. Wohlgemuth, "Evaluation of temperature and humidity on PV module component degradation," in *2013 IEEE 39th Photovoltaic Specialists Conference (PVSC)*, Jun. 2013, pp. 0120–0125.

[4] N. Bosco, T. J. Silverman, and S. Kurtz, "The Influence of PV Module Materials and Design on Solder Joint Thermal Fatigue Durability," *IEEE Journal of Photovoltaics*, vol. 6, no. 6, pp. 1407–1412, Nov. 2016.

[5] M. A. Hasan and R. A. Tarefder, "Development of temperature zone map for mechanistic empirical (ME) pavement design," *International Journal of Pavement Research and Technology*, vol. 11, no. 1, pp. 99–111, Jan. 2018. [Online]. Available: http://www.sciencedirect.com/science/article/pii/S1996681417301165

[6] D. C Jordan, J. H Wohlgemuth, and S. R Kurtz, "Technology and Climate Trends in PV Module Degradation," in *Proceedings of the 27th European Photovoltaic Solar Energy Conference and Exhibition*, Jan. 2012, pp. 3118–3124.

[7] W. K\textbackslash"{o}ppen, "Classification of climates according to temperature, precipitation and seasonal cycle," *Petermanns Geogr. Mitt*, vol. 64, pp. 193–203, 1918.

[8] S. Lindig, I. Kaaya, K. Wei, D. Moser, and M. Topic, "Review of Statistical and Analytical Degradation Models for Photovoltaic Modules and Systems as Well as Related Improvements," *IEEE Journal of Photovoltaics*, vol. 8, no. 6, pp. 1773–1786, Nov. 2018.

[9] A. Habte, M. Sengupta, C. A. Gueymard, R. Narasappa, O. Rosseler, and D. M. Burns, "Estimating ultraviolet radiation from global horizontal irradiance," *IEEE Journal of Photovoltaics*, vol. 9, no. 1, pp. 139–146, Jan 2019.

[10] O. Haillant, D. Dumbleton, and A. Zielnik, "An Arrhenius approach to estimating organic photovoltaic module weathering acceleration factors," *Solar Energy Materials and Solar Cells*, vol. 95, no. 7, pp. 1889–1895, Jul. 2011. [Online]. Available: http://www.sciencedirect.com/science/article/pii/S0927024811000936

[11] S. Kurtz, K. Whitfield, D. Miller, J. Joyce, J. Wohlgemuth, M. Kempe, N. Dhere, N. Bosco, and T. Zgonena, "Evaluation of high-temperature exposure of rack-mounted photovoltaic modules," in *2009 34th IEEE Photovoltaic Specialists Conference (PVSC)*, Jun. 2009, pp. 002 399–002 404.

[12] V. Vasudevan and X. Fan, "An acceleration model for lead-free (SAC) solder joint reliability under thermal cycling," in *2008 58th Electronic Components and Technology Conference*, May 2008, pp. 139–145.

[13] N. Bosco, T. J. Silverman, and S. Kurtz, "Climate specific thermo-mechanical fatigue of flat plate photovoltaic module solder joints," *Microelectronics Reliability*, vol. 62, pp. 124–129, Jul. 2016.

[14] N. C. Park, W. W. Oh, and D. H. Kim, *Effect of Temperature and Humidity on the Degradation Rate of Multicrystalline Silicon Photovoltaic Module*, 2013. [Online]. Available: https://www.hindawi.com/journals/ijp/2013/925280/abs/

[15] W. F. Holmgren, R. W. Andrews, A. T. Lorenzo, and J. S. Stein, "PVLIB Python 2015," in *2015 IEEE 42nd Photovoltaic Specialist Conference (PVSC)*, Jun. 2015, pp. 1–5.

[16] M. Lave, W. Hayes, A. Pohl, and C. W. Hansen, "Evaluation of Global Horizontal Irradiance to Plane-of-Array Irradiance Models at Locations Across the United States," *IEEE Journal of Photovoltaics*, vol. 5, no. 2, pp. 597–606, Mar. 2015.

[17] D. G. Erbs, S. A. Klein, and J. A. Duffie, "Estimation of the diffuse radiation fraction for hourly, daily and monthly-average global radiation," *Solar Energy*, vol. 28, no. 4, pp. 293–302, Jan. 1982. [Online]. Available: http://www.sciencedirect.com/science/article/pii/0038092X82903024

[18] D. King, W. Boyson, and J. Kratochvil, "Photovoltaic Array Performance Model," Sandia National Laboratories, Albuquerque, NM, Tech. Rep. SAND2004-3535, 2004.